

A Theoretical Study on Pd^{II} Complexes Containing Hemilabile Pyrazole-Derived Ligands

Albert Rimola,^[a] Mariona Sodupe,^{*[a]} Josep Ros,^[a] and Josefina Pons^{*[a]}

Keywords: Pd^{II} complexes / Pyrazole / Hemilabile ligands / Density functional theory

The properties of Pd^{II} complexes containing hemilabile pyrazole-derived ligands (L) of the form BPz-(CH₂)_x-A(CH₂)_y-A(CH₂)_x-PzB, with A being a donor atom and B a substituent group at the pyrazole ring, have been investigated through quantum-chemical calculations. The geometries of the [PdLCl₂] and [PdL]²⁺ complexes have been optimized and the reaction free energy of [PdLCl₂] → [PdL]²⁺ + 2 Cl⁻ computed for 32 different ligands, using the hybrid B3LYP density functional method. The formation of the tetra-coordinate [PdL]²⁺ complexes is more favorable for the

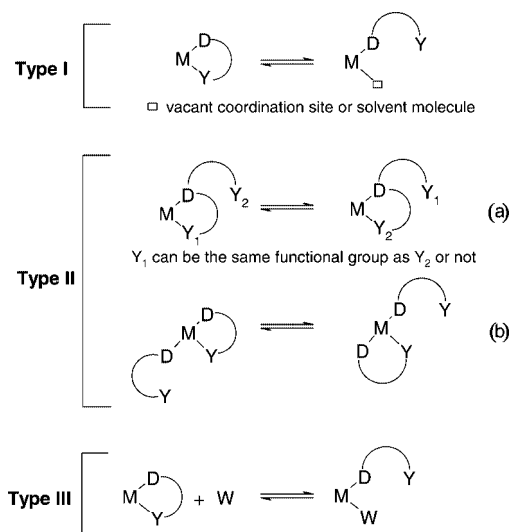
longer (eight- and nine-membered) chains than for the shorter (six- and seven-membered) ones. Moreover, results show the nature of the donor atom A influences significantly the formation of [PdL]²⁺, the process becoming more favorable according to the order PH > NH > S > O. Finally, electron-donor substituents at the pyrazole ring enhance the formation of [PdL]²⁺, whereas electron-acceptor groups hinder the process.

(© Wiley-VCH Verlag GmbH & Co. KGaA, 69451 Weinheim, Germany, 2006)

Introduction

The study of hemilabile ligands has received an increasing interest in recent years. The main reason for this attention is the capability of hemilabile ligands to generate vacant coordination sites and to stabilize reaction intermediates which result in promising chemical properties. The relevance and utility of this concept gave rise to the publication of excellent reviews which cover all the aspects of these ligands.^[1] The term “hemilabile” was first introduced by Jeffrey and Rauchfuss in 1979, and it refers to polidentate coordination ligands which possess at least one substitutionally labile donor function.^[2] There are several examples in the literature about the influence of transition-metal complexes with hemilabile ligands in the activation of small molecules^[3–6] and in the activity of homogeneous catalysis.^[7–9] Furthermore, hemilability probably occurs also in other disciplines such as bioinorganic chemistry or surface phenomena. A very useful classification of hemilabile situations was reported by Braunstein and Naud in an excellent review.^[10] According to these authors three general types of hemilability can be visualized (see Scheme 1). Hemilability of type I is found when the labile donor group coordinates and decoordinates spontaneously. In hemilability of type II there is an intramolecular competition between the donor groups in the same ligand (a) or between donor groups of two identical ligands (b). Finally, hemilability of type III

refers to a situation where there is a competition between a labile donor center and an external solvent molecule. Although this phenomenon was first studied in mononuclear complexes, it has been expanded to dinuclear^[11] and polynuclear ones, particularly to metal clusters.^[12] It should be pointed out that, although homofunctional bidentate ligands such as R₂N(CH₂)_nNR₂ or R₂P(CH₂)_nPR₂ could coordinate in monodentate or bidentate forms, they are not considered hemilabile since their coordination mode depends on the metal center and the effects of the coordinated ligands. In fact, hybrid ligands containing very different do-



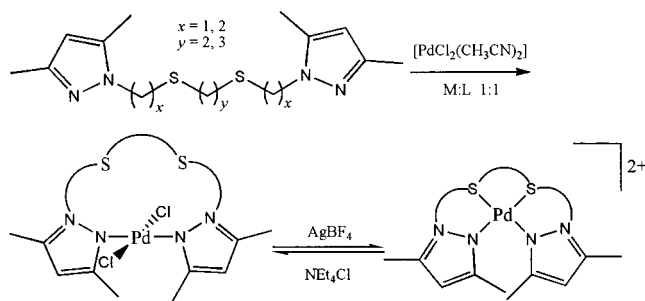
Scheme 1.

[a] Departament de Química, Universitat Autònoma de Barcelona, 08193 Bellaterra, Spain
E-mail: Mariona.Sodupe@uab.es
Josefina.Pons@uab.es

Supporting information for this article is available on the WWW under <http://www.eurjic.org> or from the author.

nor functions, such as hard and soft donor atoms, are the basis of most of hemilabile ligands.

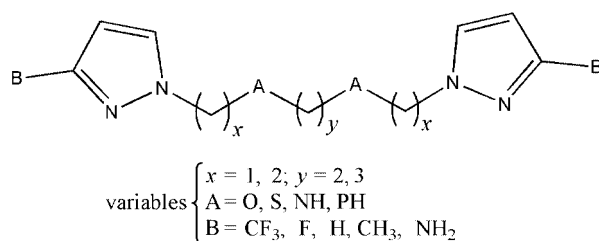
Pyrazole-derived ligands are potential hemilabile ligands since steric and electronic properties of both the pyrazole and the ancillary donor groups can be easily tuned.^[13] In recent years our research group has reported the synthesis, the characterization and the coordinating properties of pyrazolic ligands containing additional donor groups: N,N,^[14] N,O,^[15] N,P^[16] and N,S.^[17] NMR studies of complexes in solution have shown that some of them display hemilability; pyrazole is the stronger (inert) donor group, except in the case of N,P and N,S for which it can also behave as a labile group. Previous studies with Pz-(CH₂)_xS(CH₂)_yS(CH₂)_x-Pz tetradentate ligands and Pd^{II} have shown that both N,N bicoordination and N,S,S,N tetracoordination are obtained and can be interconverted in solution (see Scheme 2).^[17c] Moreover, the formation of the N,S,S,N coordinating mode in Pd^{II} complexes appears to be controlled by the geometry imposed by the PdNNCS ring in such a manner that ligands Pz-(CH₂)_xS(CH₂)_yS(CH₂)_x-Pz with $x = 1$ did not lead to the formation of the tetradentate coordination. However, the N,S,S,N complex was obtained for different lengths of the alkyl chain between S atoms ($y = 1, 2$). This interesting observation can be visualized as a recognition phenomenon of the planar Pd^{II} ion by the N,S,S,N ligand which would act as a chemical receptor. Given that the selective metal ion recognition plays a fundamental role in the search of chemical and biochemical sensors^[18] the combination of both strong and weak donor centers found in the same pyrazole–thioether receptor might open new perspectives in the applications of hemilabile ligands. Some molecular recognition processes involving Pd^{II} complexes were described in the literature.^[19,20]



Scheme 2.

The main goal of this paper is to perform a comprehensive theoretical study on the properties of pyrazole-containing ligands (L) of the form BPz-(CH₂)_xA(CH₂)_yA(CH₂)_x-PzB, with A being a donor atom and B a substituent group at the pyrazole ring, through quantum-chemical calculations (Scheme 3). For that, we have optimized the geometry of the [PdCl₂L] and [PdL]²⁺ complexes and computed the reaction free energy of [PdCl₂L] → [PdL]²⁺ + 2 Cl⁻, for 32 different ligands. This study has allowed us to analyze the influence of the number of -CH₂- groups that join the two pyrazole rings, the nature of donor atoms directly bonded

to Pd in the products, and the electronic effects induced by substituent groups at the pyrazole rings.



Scheme 3.

Results and Discussion

As mentioned, the labile behavior of the ligands exposed in the introduction is given by the thioether groups, the inert groups being the pyrazole rings. This labile behavior varies depending on the number of -CH₂- groups that join the two pyrazole rings (variables x and y), but it can also be modified by other factors, such as the nature of the donor atom that is directly bonded to Pd in the products (variable A), and the electronic effects induced by substituent groups at the pyrazole rings (variable B). All these variables, labeled in Scheme 3, affect the electronic and the structural properties of the complexes and, consequently, the hemilabile equilibrium [PdCl₂L] ⇌ [PdL]²⁺ + 2 Cl⁻. Free-energy calculations for this reaction with all ligands built with these variables show that there is a clear relationship between the energetic results and the structural factors.

I. Chain Length

Ligands with different chain lengths have been built by changing the values of variables x and y . We have considered six- ($x = 1, y = 2$), seven- ($x = 1, y = 3$), eight- ($x = 2, y = 2$), and nine-membered ($x = 2, y = 3$) chains. To make the discussion less tedious, hereafter, these systems will be referred to as hexane-, heptane-, octane-, and nonane-chain systems. In all cases, the other variables have been kept fixed to A = S and B = CH₃. Since the length of the chain mainly influences the geometry of the reaction products, only the optimized structures of [PdL]²⁺ complexes are shown in Figure 1.

It can be observed that the bond lengths of the newly formed Pd–S bonds show significant deviations (about 0.06 Å) upon increasing the chain length. More importantly, the square-planar coordination of Pd in [PdL]²⁺ can be significantly distorted depending on the length of the ligand. In particular, it is observed that hexane- and heptane-chain systems present N–Pd–N *cis* angles (102°–108°) that are much larger than the N–Pd–S *cis* ones (81°–82°), whereas in octane and nonane structures the computed N–Pd–N *cis* angles (90°–95°) are much closer to the N–Pd–S ones (88°–89°). On the other hand, the N–Pd–S *trans* angles tend to 180° and the deviation from planarity decreases^[21]

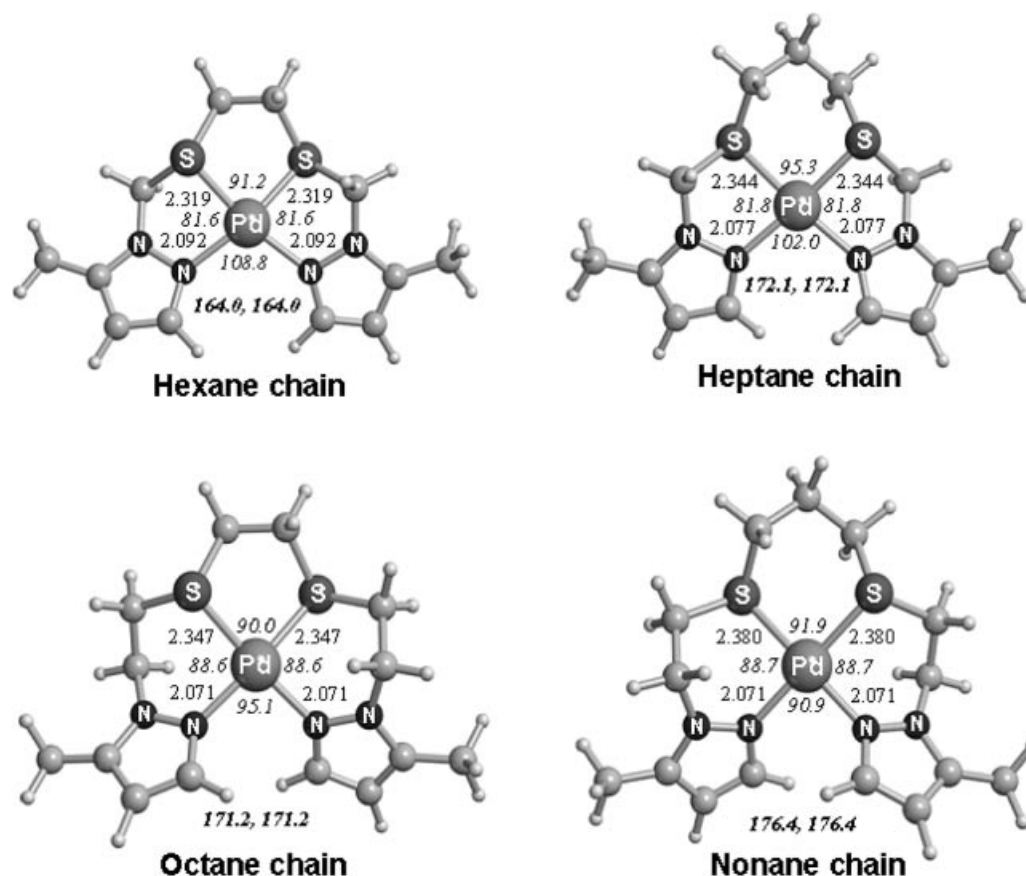


Figure 1. Main geometry parameters optimized at the B3LYP level. Distances are in Å and angles in degrees. Standard numbers correspond to distances, italic numbers to *cis* angles, and bold and italic numbers to *trans* angles.

as the chain length is increased. Therefore, we can conclude that, compared to the ideal square-planar geometry, products with six- and seven-membered chains are more distorted than those with eight- and nine-membered chains. This can be related to the type of rings formed in products. In the hexane-chain products, we obtain three five-membered rings, in the heptane-chain ones two five-membered rings and one six-membered ring, in the octane-chain complexes one five and two six-membered rings and, finally, in nonane-chain products all three rings are six-membered. These results seem to suggest that formation of five-membered rings introduce important strain in the complex that leads to quite distorted structures with respect to the ideal square-planar geometry. Computed structural parameters are in a good agreement with the crystallographic data of related complexes synthesized.^[17c]

Reaction free energies have been calculated both in the gas phase and in solution. Calculations in solution have been performed using the conductor-like COSMO continuum model^[27] with three different solvents: CH₃OH ($\epsilon = 32.63$), acetone ($\epsilon = 20.70$), and CH₂Cl₂ ($\epsilon = 8.93$). Results are given in Figure 2. As expected, the computed free energy of the $[\text{PdLCl}_2] \rightarrow [\text{PdL}]^{2+} + 2 \text{Cl}^-$ reaction is much smaller in solution than in the gas phase and decreases when the dielectric constant of the solvent increases due to the enhanced stability of the charged species. Nevertheless,

in all cases the trends observed upon enlarging the chain length are the same; i.e. the reaction is favored from the hexane- to the nonane-chain ligand, the reaction energy decreasing by 23–29 kcal/mol. Since product complexes are the ones that suffer larger structural changes due to the length of the chain, the reaction free energies are expected to be governed by the stability of the products. In principle, it is possible to distinguish two different groups: i) the six-

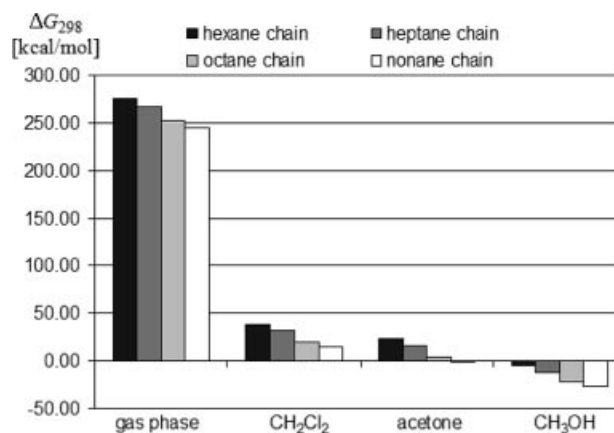


Figure 2. Computed reaction free energies (ΔG_{298}) of $[\text{PdLCl}_2] \rightarrow [\text{PdL}]^{2+} + 2 \text{Cl}^-$ in the gas phase and in solution. In kcal/mol. Effect of chain length.

and seven-membered chain complexes, and ii) the eight- and nine-membered ones, the reaction energies for the latter species being energetically more favorable. These two groups are the same observed when the structural factors were considered. So, there is a clear trend: the more distorted the products are, the more the equilibrium favors the reactants. These theoretical results agree with the experimental data which show that product complexes with octane- and nonane-chain ligands can be synthesized, whereas those with hexane- and heptane-chain ligands are not observed^[17c].

II. Donor Atom

The changes produced on the structural parameters have been analyzed for four different donor atoms $A = O, S, NH,$ and PH . We have optimized all the structures built with the values $x = 1, 2; y = 2, 3$; and $B = CH_3$. Table 1 shows the optimized $Pd-N_{\text{azine}}$ and $Pd-A$ distances, both for reactants and products.

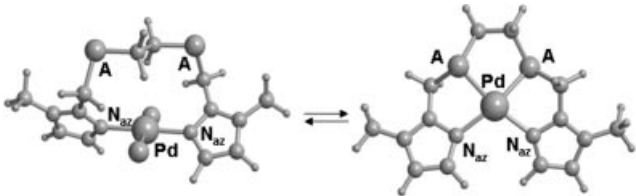
For reactants, all $Pd-N_{\text{azine}}$ distances are similar (2.06–2.07 Å). This is not surprising considering that the chain length does not affect the $Pd-NH$ interaction and that the donor atoms are not interacting with Pd in the reactant complexes $[PdLCl_2]$. In contrast, the $Pd-N_{\text{azine}}$ distances range from 2.01 to 2.15 Å in the product complexes $[PdL]^{2+}$. The longest $Pd-N_{\text{azine}}$ distances appear for species with PH , followed by those with S, NH , and finally O , which shows the shortest distance. Furthermore, for ligands with PH and S , the $Pd-N_{\text{azine}}$ bond lengths increase as the reaction proceeds, whereas for ligands with NH and O , these distances decrease. That is, the formation of the two new $Pd-A$ bonds weakens the $Pd-N_{\text{azine}}$ interaction for $A = PH$ and S and strengthens it for $A = O$ and NH . The other structural parameters such as *cis* and *trans* angles are not affected by the effects of the different donor atoms.

In order to obtain a deeper insight into the hemilabile character of these ligands we have used Bader's theory of

"Atoms in Molecules".^[22] In this work we have computed the values of $\rho(r)$ (electron charge density at the bond critical point, bcp), the values of $\nabla^2\rho(r)$ (Laplacian of the electron charge density at the bcp that coincides with the sum of the three curvatures of the Hessian matrix), and the ratio $|\lambda_1/\lambda_3|$ (λ_i being the curvatures of the Hessian matrix) at the $Pd-N_{\text{azine}}$ and $Pd-A$ bcp. According to this theory, values of $\nabla^2\rho(r) < 0$ address regions where the charge density is concentrated. In contrast, regions in which $\nabla^2\rho(r) > 0$, the charge density is depleted. The ratio of $|\lambda_1/\lambda_3|$ is a measure of the covalency between two atoms. Ratios greater than unity indicate covalent or polar interactions, usually referred to as shared interactions. Ratios lower than 0.2 imply closed-shell interactions, such as those given in noble gas repulsive states, in ionic bonds, in hydrogen bonds, and in van der Waals molecules.^[22b]

The $\rho(r)$ values at the $Pd-N_{\text{azine}}$ bcp, both in reactants and products, are shown in Figure 3. In agreement with the computed $Pd-N_{\text{azine}}$ distances, the computed electron density values in the reactants remain similar (between 0.093 and 0.096), regardless of the donor atom. However, in the products these values range from 0.111 to 0.081 and follow the sequence $O > NH > S > PH$. On the other hand, it can be observed in Figure 3 that when S is a donor atom, the electron density value at the $Pd-N_{\text{azine}}$ bcp is similar in reactants and products. Considering that in the reactants the $Pd-N_{\text{azine}}$ bond is in *trans* position with another $Pd-N_{\text{azine}}$ bond, and that in the products the $Pd-N_{\text{azine}}$ bonds are in *trans* position with the newly formed $Pd-S$ bonds, this seems to suggest that the N_{azine} and S donor atoms have a similar donor character and that the $Pd-N_{\text{azine}}$ and $Pd-S$ bonds are similar in strength. For NH and O , the electron density values of $Pd-N_{\text{azine}}$ at the bond critical points increase as the reaction proceeds. Therefore, the N_{azine} atoms exert a *trans* influence on NH and O donor atoms. In contrast, when PH acts as donor atom, the electron density values of $Pd-N_{\text{azine}}$ bond critical points decrease along the reaction because PH exerts a *trans* influ-

Table 1. $Pd-N_{\text{azine}}$ and $Pd-A$ distances in $[PdLCl_2]$ and $[PdL]^{2+}$. Distances are in Å.



		Hexane chain		Heptane chain		Octane chain		Nonane chain	
		Reactant	Product	Reactant	Product	Reactant	Product	Reactant	Product
O	$Pd-N_{\text{azine}}$	2.063	2.030	2.065	2.019	2.061	2.014	2.062	2.024
	$Pd-A$		2.060		2.097		2.096		2.125
N	$Pd-N_{\text{azine}}$	2.061	2.056	2.064	2.044	2.058	2.045	2.062	2.064
	$Pd-A$		2.057		2.096		2.104		2.113
S	$Pd-N_{\text{azine}}$	2.069	2.092	2.066	2.077	2.058	2.071	2.061	2.071
	$Pd-A$		2.319		2.344		2.353		2.380
P	$Pd-N_{\text{azine}}$	2.059	2.153	2.070	2.127	2.057	2.122	2.062	2.119
	$Pd-A$		2.244		2.264		2.285		2.308

ence on N_{azine}. According to these results, the strength of the Pd–A bonds seems to follow the order Pd–PH > Pd–S > Pd–NH > Pd–O.

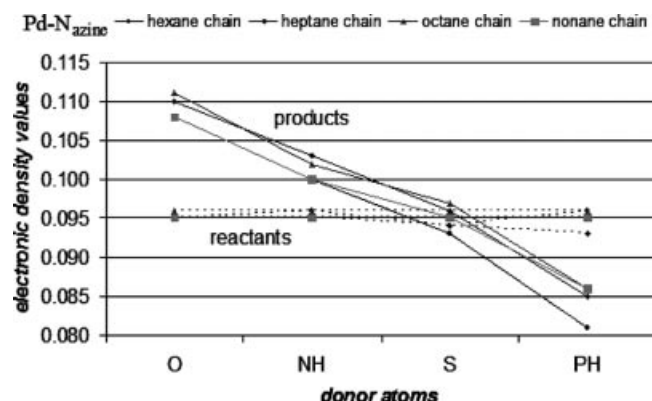


Figure 3. $\rho(r)$ density values at the Pd–N_{azine} bond critical points in reactants, PdLCl₂, and products, PdL²⁺. Effect of donor atoms.

The computed values of $\rho(r)$, $\nabla^2\rho(r)$, and $|\lambda_1/\lambda_3|$ at the Pd–N_{azine} and Pd–A bond critical points as well as the net atomic charge of Pd^{II} for nonane-chain products are summarized in Table 2. The fact that the values obtained for $\nabla^2\rho(r)$ at the bcp for Pd–N_{azine} are positive and relatively large evidence a closed-shell interaction. This fact is reinforced by the values of $|\lambda_1/\lambda_3|$, which are lower than 0.2. Regarding the Pd–A bcp, it is worth to note an interesting tendency in the nature of the interaction. From the beginning to the end of the series O, NH, S, PH, the values of $\nabla^2\rho(r)$ decrease and the $|\lambda_1/\lambda_3|$ ratio increases. This fact means that the shared interaction between Pd and the donor atoms follows the order Pd–O < Pd–NH < Pd–S < Pd–PH. This tendency is confirmed by the values of the net atomic charge of Pd, which indicate that the charge transfer from the donor atoms to Pd increases according to the same order. These results agree with the trends observed by the *trans* influence. According to them one would expect that the formation of the new Pd–A bonds would become energetically more favorable as we go from O to NH, from NH to S, and from S to PH.

Table 2. Electron density, $\rho(r)$, Laplacian, $\nabla^2\rho(r)$ and $|\lambda_1/\lambda_3|$ values at the Pd–N_{azine} and Pd–A bond critical points, and Pd net atomic charge.

	Pd–N _{azine}			Pd–A			Charge
	ρ	$\nabla^2\rho$	$ \lambda_1/\lambda_3 $	ρ	$\nabla^2\rho$	$ \lambda_1/\lambda_3 $	
O	0.108	0.449	0.176	0.074	0.390	0.139	0.92
N	0.100	0.432	0.170	0.081	0.334	0.175	0.79
S	0.095	0.410	0.173	0.086	0.174	0.224	0.58
P	0.086	0.372	0.169	0.100	0.092	0.331	0.43

The computed reaction free energies of [PdLCl₂] → [PdL]²⁺ + 2 Cl[–] are given in Figure 4. We only report the values in the gas phase since both results in the gas phase and in solution follow the same trends (see above). It can be observed that the computed free energies do not follow the expected order as shown in Figure 4: $\Delta G(O) > \Delta G(S) > \Delta G(NH) > \Delta G(PH)$. That is, the reaction appears to be

more favorable for ligands with NH than for those with S. To obtain a deeper insight into the reaction driving force, we have split the reaction energy ($\Delta E_{\text{reaction}}$) in two terms: i) the difference between the interaction energies in reactants and products (ΔE_{int}) and ii) the reorganization energy (ΔE_{reorg}) of the ligand. The interaction energy in the reactants ($E_{\text{int(React)}}$) corresponds to $E(\text{PdLCl}_2) - E(\text{Pd}^{\text{II}}) - E(\text{L}) - 2 E(\text{Cl}^-)$, whereas that in the products ($E_{\text{int(Prod)}}$) is $E(\text{PdL}^{2+}) - E(\text{Pd}^{\text{II}}) - E(\text{L})$. The term ΔE_{reorg} can be understood as the energy cost associated to the conformational change of the ligand along the reaction, and corresponds to the energy difference between single-point calculations of the ligand at the geometry of reactants and products. The values of these terms are shown in Table 3 for the nonane chains. Since $E_{\text{int(React)}}$ is quite constant for all systems and variations in ΔE_{reorg} are small, the main contribution on the reaction energy comes from $E_{\text{int(Prod)}}$, which follows the same trend of $\Delta E_{\text{reaction}}$ and ΔG_{298} (see Figure 4). It is worth noting that the largest reorganization energy is obtained for PH ligands. This is probably related to the higher barrier for inversion at P. Despite that, reactions with this donor atom are the most favored ones. The order obtained for the interaction energies in the products (PH > NH > S > O; in absolute values) is the same as that found for the interaction between Pd^{II} and the smallest donor-atom-containing entities H₂O, H₂S, NH₃, and PH₃ (–141.6, –180.5, –192.1, and –211.8 kcal/mol, respectively) and arises from different factors: electrostatic interaction, metal–ligand repulsion, and charge transfer. As expected, population analysis indicates that the charge transfer from the ligand to Pd is larger for S and PH species than for O and NH ones. However, a point-charge model assuming a 2+ charge at the Pd position shows that the electrostatic stabilization is larger for NH₃ and PH₃ than for H₂O and H₂S. As a consequence, the preference of Pd^{II} to interact with donor atoms follows the order PH > NH > S > O. These results agree with the experimental fact that the inert groups of hemilabile ligands contain P atoms while the labile ones contain O atoms.^[1]

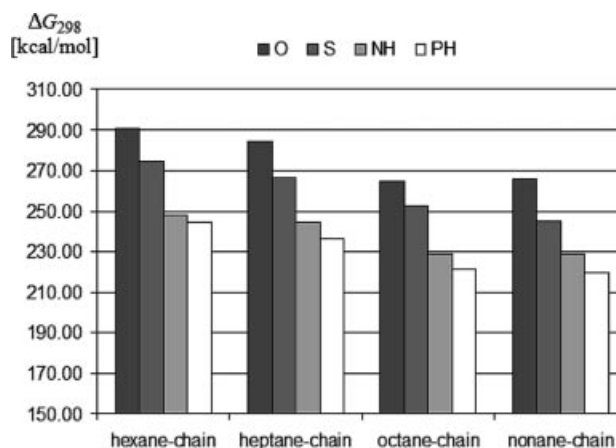


Figure 4. Computed reaction free energies (ΔG_{298}) of PdLCl₂ → PdL²⁺ + 2 Cl[–] in the gas phase. In kcal/mol. Effect of donor atoms.

Table 3. Contribution of metal-ligand interaction energies and reorganization energy of the ligand to the $[\text{PdLCl}_2] \rightarrow [\text{PdL}]^{2+} + 2 \text{Cl}^-$ reaction energy. In kcal/mol.

	$E_{\text{int(React)}}^{[a]}$	$E_{\text{int(Prod)}}^{[b]}$	$\Delta E_{\text{int}}^{[c]}$	$\Delta E_{\text{reorg}}^{[d]}$	$\Delta E_{\text{reaction}}$
O	-692.3	-437.4	254.9	25.5	280.4
S	-692.1	-454.5	237.6	22.8	260.4
N	-692.6	-478.4	214.2	25.9	240.0
P	-692.6	-501.3	191.4	40.8	232.2

[a] $E_{\text{int(React)}} = E(\text{PdLCl}_2) - E(\text{Pd}^{\text{II}}) - E(\text{L}) - 2 E(\text{Cl}^-)$.

[b] $E_{\text{int(Prod)}} = E(\text{PdL}^{2+}) - E(\text{Pd}^{\text{II}}) - E(\text{L})$. [c] $\Delta E_{\text{int}} = E_{\text{int(Prod)}} - E_{\text{int(React)}}$. [d] $\Delta E_{\text{reorg}} = E(\text{L})_{\text{Prod}} - E(\text{L})_{\text{React}}$.

C. Ring Substituents

Substituents with different electronic properties ($\text{B} = \text{CF}_3$, F, H, CH_3 , and NH_2) are introduced at position 5 of pyrazole rings in order to analyze their influence on the structural parameters of Pd complexes and on the $[\text{PdLCl}_2] \rightarrow [\text{PdL}]^{2+} + 2 \text{Cl}^-$ reaction. Calculations have been performed for different chain lengths ($x = 1, 2$ and $y = 2, 3$) and assuming S as donor atom. Table 4 shows the optimized $\text{Pd}-\text{N}_{\text{azine}}$ bond lengths, both for reactants and products.

It can be observed that changing the substituent at the pyrazole ring does not induce a significant variation on the $\text{Pd}-\text{N}_{\text{azine}}$ bond length of the reactant complexes. This is due to the fact that ring pyrazoles are in the *trans* configuration, and thus the electronic effects of the substituents are mutually compensated. However, the $\text{Pd}-\text{N}_{\text{azine}}$ bond lengths in the products are longer when substituents have a global electron-withdrawing character. The contrary occurs if substituents have a global electron-donor character, the $\text{Pd}-\text{N}_{\text{azine}}$ distances becoming shorter. Nevertheless, the $\text{Pd}-\text{S}$ bonds are not affected by the type of substituent.

We have also calculated the electron density values of the $\text{Pd}-\text{N}_{\text{azine}}$ bond critical points in the products, and the results are shown in Figure 5. The observed trends agree with the observed changes on the $\text{Pd}-\text{N}_{\text{azine}}$ distances; that is, products with electron-withdrawing substituents (and longer $\text{Pd}-\text{N}_{\text{azine}}$ bonds), present smaller electron density values at the bond critical points than product complexes

with electron-donor substituents (and shorter $\text{Pd}-\text{N}_{\text{azine}}$ distances). Based on these results the variation on the $\text{Pd}-\text{N}_{\text{azine}}$ bond strength, due to the effects of substituents, is expected to follow the order $\text{CH}_3 > \text{NH}_2 > \text{H} > \text{F} > \text{CF}_3$.

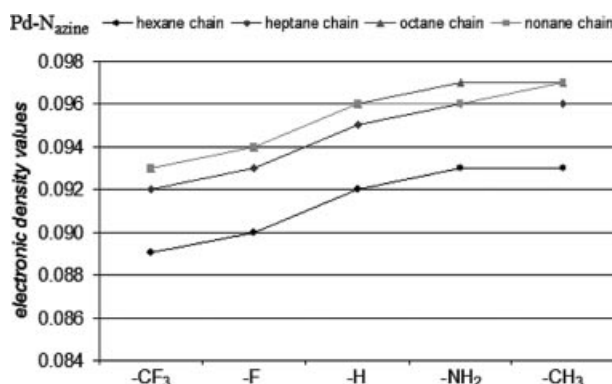
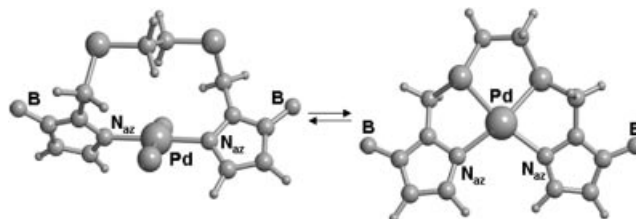


Figure 5. $\rho(r)$ density values at the $\text{Pd}-\text{N}_{\text{azine}}$ bond critical points in products, $[\text{PdL}]^{2+}$. Effect of ring substituent.

The induced structural and electronic changes will influence the stability of the products and consequently, the $[\text{PdLCl}_2] \rightarrow [\text{PdL}]^{2+} + 2 \text{Cl}^-$ reaction energy. Gas-phase reaction free energies calculated for the different ligands considered are given in Figure 6. As expected, reactions are more favored when substituents have an electron-donor character, in agreement with the changes observed for the $\text{Pd}-\text{N}_{\text{azine}}$ bond lengths and electron density values at the bond critical point. However, the trends on $\text{Pd}-\text{N}_{\text{azine}}$ bond length or electron density values do not perfectly agree with the observed trends in reaction free energies. That is, whereas with CH_3 as substituent the $\text{Pd}-\text{N}_{\text{azine}}$ distances are shorter than with NH_2 , the reaction is more favorable if the substituent is NH_2 . This may be understood considering that, in addition to the σ -donor electronic character, NH_2 has a π -donor resonant character that enhances more the global stability of the products. It is worth noting that the reaction free energy can change by as much as 27–29 kcal/mol by introducing substituents of different character in the pyrazole ring.

Table 4. $\text{Pd}-\text{N}_{\text{azine}}$ distances in $[\text{PdLCl}_2]$ and $[\text{PdL}]^{2+}$. Distances are in Å.

	Hexane chain		Heptane chain		Octane chain		Nonane chain	
B	Reactant	Product	Reactant	Product	Reactant	Product	Reactant	Product
CF_3	2.071	2.111	2.071	2.094	2.059	2.087	2.063	2.084
F	2.066	2.105	2.067	2.088	2.056	2.080	2.059	2.079
H	2.067	2.098	2.067	2.082	2.058	2.075	2.060	2.075
NH_2	2.071	2.093	2.065	2.077	2.060	2.075	2.059	2.074
CH_3	2.069	2.092	2.066	2.077	2.058	2.071	2.061	2.071



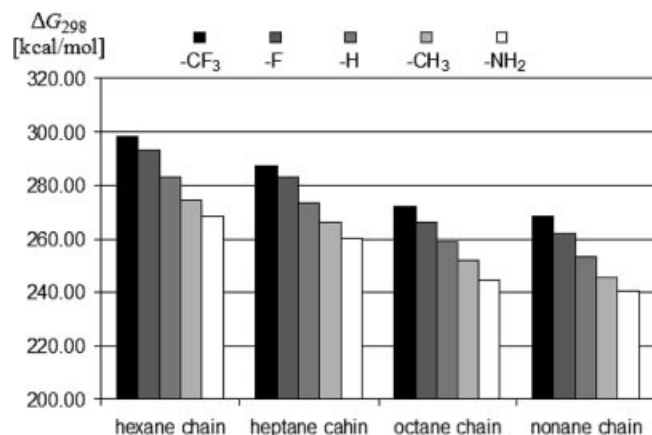


Figure 6. Computed reaction free energies (ΔG_{298}) of $[\text{PdLCl}_2] \rightarrow [\text{PdL}]^{2+} + 2 \text{Cl}^-$ in the gas phase. In kcal/mol. Effect of ring substituents.

Conclusions

The properties of Pd^{II} complexes containing pyrazole-derived hemilabile ligands BPz-(CH₂)_xA(CH₂)_yA(CH₂)_x-PzB (with $x = 1, 2$; $y = 2, 3$; A = O, NH, S and PH; and B = CF₃, F, H, CH₃, NH₂) have been investigated through quantum-chemical calculations. Optimal geometries for $[\text{PdLCl}_2]$ and $[\text{PdL}]^{2+}$ complexes and the reaction free energy of $[\text{PdCl}_2\text{L}] \rightarrow [\text{PdL}]^{2+} + 2 \text{Cl}^-$ have been determined for 32 different ligands using the hybrid B3LYP density functional method. Compared to the ideal square-planar geometry, products with six- ($x = 1$, $y = 2$) and seven-membered ($x = 2$, $y = 3$) chains are more distorted than those with eight- ($x = 2$, $y = 2$) and nine-membered ($x = 2$, $y = 3$) chains. Thus, formation of tetracoordinate $[\text{PdL}]^{2+}$ complexes is more favorable for the longer chains. This is in agreement with the experimental results, which show that only octane and nonane ligand complexes can be isolated and characterized. Results for different donor atoms A show that the $[\text{PdCl}_2\text{L}] \rightarrow [\text{PdL}]^{2+} + 2 \text{Cl}^-$ reaction is favoured according to the order PH > NH > S > O. This seems to contradict the electron density analysis which shows a larger L→Pd^{II} charge transfer for A = S than for A = NH. The reaction energy decomposition and point charge calculations show, however, that the electrostatic + polarization stabilizing term is larger when A = NH. Finally, the introduction of substituents at the pyrazole ring can modulate the strength of the Pd–N_{azine} bond and modify the reaction energy, the electron-donor substituents enhancing the formation of $[\text{PdL}]^{2+}$.

Theoretical Details

Molecular geometries were optimized using the non-local hybrid three-parameter B3LYP^[23] density functional method with the Gaussian98 program package.^[24] Frequency calculations were also performed to confirm that each stationary point is an actual minimum. For Pd we used the quasi-relativistic effective core potential (ECP) of Hay and Wadt^[25] to represent the 28 innermost electrons of the palladium atom. The basis set used for the valence and out-

ermost core orbitals is the standard double- ζ LANL2DZ set associated to the ECP. For atoms directly attached to the metal atom (Cl, N_{azine}, and the heteroatoms O, N, S, and P from the ligand chain) we used the 6-31++G(d,p) basis,^[26] whereas the remaining atoms were described with the smaller 6-31G basis.^[27] In order to analyze the influence of further enlarging the basis set on the $\text{PdLCl}_2 \rightarrow \text{PdL}^{2+} + 2 \text{Cl}^-$ reaction energy, we have also performed (for a few cases) single-point calculations by adding an f function to the Pd basis,^[28] and using the 6-311++G(2d,2p) basis sets for the atoms directly bonded to the metal center. Results showed that the reaction energies differ by less than 1 kcal/mol and thus, we expect computed reaction energies with the small basis set to be reasonably accurate. Thermodynamic corrections have been obtained by standard statistical methods, assuming the harmonic/rigid rotor approximation.^[29] Solvent effects have been introduced using the Conductor-like Screening Model (COSMO) method,^[30] by performing single-point calculations at the gas-phase-optimized geometries. Net atomic charges have been obtained using the natural population analysis (NPA) method of Weinhold et al.^[31] while the topological properties of the electron density have been studied employing Bader's theory of "Atoms In Molecules" (AIM)^[22] by means of the Xaim software.^[32]

Supporting Information (see footnote on the first page of this article): Optimized geometries (Cartesian coordinates) of all considered $[\text{PdLCl}_2]$ and $[\text{PdL}]^{2+}$ complexes.

Acknowledgments

Financial support from MCYT and FEDER (project BQU2002-04112-C02), DURSI (projects 2001SGR-00182 and 2001SGR-00290), and the use of the computational facilities of the Catalonia Supercomputer Center (CESCA) are gratefully acknowledged. M. S. A. R. is indebted to the Universitat Autònoma de Barcelona for a doctoral fellowship.

- [1] For reviews on hemilabile ligands see: a) A. Bader, E. Lindner, *Coord. Chem. Rev.* **1991**, 108, 27; b) E. Lindner, S. Pautz, M. Hausteine, *Coord. Chem. Rev.* **1996**, 155, 145; c) C. S. Slone, D. A. Weinberger, C. A. Mirkin, *Prog. Inorg. Chem.* **1999**, 48, 233; d) P. Espinet, K. Soulantica, *Coord. Chem. Rev.* **1999**, 147, 1; e) L. Pascale, N. Le Bris, H. des Abbayes, *Trends Organomet. Chem.* **2002**, 4, 131; f) U. Shubert, J. Pfeiffer, F. Stohr, D. Sturm, S. Thompson, *J. Organomet. Chem.* **2002**, 646, 53; g) P. Braunstein, *J. Organomet. Chem.* **2004**, 689, 3953.
- [2] J. C. Jeffrey, T. B. Rauchfuss, *Inorg. Chem.* **1979**, 18, 2658.
- [3] E. Poverenov, M. Gandelman, L. J. W. Shimon, H. Rozenberg, Y. Ben-David, D. Milstein, *Organometallics* **2005**, 24, 1082.
- [4] M. Basseti, P. Alvarez, J. Gimeno, E. Lastra, *Organometallics* **2004**, 23, 5127.
- [5] M. Basseti, A. Capone, M. Salamone, *Organometallics* **2004**, 23, 247.
- [6] H. Werner, *Dalton Trans.* **2003**, 3829.
- [7] J. Heinicke, M. Koehler, N. Peuleke, M. K. Kinderman, W. Keim, M. Koeckerling, *Organometallics* **2005**, 24, 344.
- [8] J. A. Brito, M. Gomez, G. Muller, H. Teruel, J. C. Clinet, E. Dunach, M. A. Maestro, *Eur. J. Inorg. Chem.* **2004**, 4278.
- [9] M. Dieguez, O. Pamies, A. Ruiz, Y. Diaz, S. Castillon, C. Claver, *Coord. Chem. Rev.* **2004**, 248, 2165.
- [10] P. Braunstein, F. Naud, *Angew. Chem. Int. Ed.* **2001**, 40, 680.
- [11] P. Braunstein, M. Knorr, C. Stern, *Coord. Chem. Rev.* **1998**, 178–180, 903.
- [12] J. A. Cabeza, *Eur. J. Inorg. Chem.* **2002**, 1559.
- [13] For reviews on pyrazole ligands see: a) S. Trofimenko, *Chem. Rev.* **1972**, 72, 497; b) S. Trofimenko, *Prog. Inorg. Chem.* **1986**, 34, 115; c) S. Trofimenko, *Chem. Rev.* **1993**, 93, 943; d) G.

- La Monica, G. A. Ardizzoia, *Prog. Inorg. Chem.* **1997**, 46, 151; e) R. Mukherjee, *Coord. Chem. Rev.* **2000**, 203, 151.
- [14] a) G. Esquiús, J. Pons, R. Yañez, J. Ros, *J. Organomet. Chem.* **2001**, 619, 14; b) G. Esquiús, J. Pons, R. Yañez, J. Ros, R. Mathieu, B. Donnadieu, N. Lugan, *Eur. J. Inorg. Chem.* **2002**, 2999; c) R. Mathieu, G. Esquiús, N. Lugan, J. Pons, J. Ros, *Eur. J. Inorg. Chem.* **2001**, 2683; d) G. Aullon, G. Esquiús, A. Lledos, F. Maseras, J. Pons, J. Ros, *Organometallics* **2004**, 23, 5530.
- [15] a) Boixassa, J. Pons, A. Virgili, X. Solans, M. Font-Bardia, J. Ros, *Inorg. Chim. Acta* **2002**, 340, 49; b) A. Boixassa, J. Pons, X. Solans, M. Font-Bardia, J. Ros, *Inorg. Chim. Acta* **2003**, 346, 151; c) A. Boixassa, J. Pons, X. Solans, M. Font-Bardia, J. Ros, *Inorg. Chim. Acta* **2003**, 355, 254; d) A. Boixassa, J. Pons, X. Solans, M. Font-Bardia, J. Ros, *Inorg. Chim. Acta* **2003**, 357, 733; e) A. Boixassa, J. Pons, J. Ros, R. Mathieu, N. Lugan, *J. Organomet. Chem.* **2003**, 682, 233; f) A. Boixassa, J. Pons, X. Solans, M. Font-Bardia, J. Ros, *Inorg. Chim. Acta* **2004**, 357, 827.
- [16] a) R. Tribo, J. Pons, R. Yañez, J. F. Piniella, A. Alvarez-Larena, J. Ros, *Inorg. Chem. Commun.* **2000**, 3, 545; b) R. Tribo, J. Ros, J. Pons, R. Yañez, A. Alvarez-Larena, J. F. Piniella, *J. Organomet. Chem.* **2003**, 676, 38; c) G. Esquiús, J. Pons, R. Yañez, J. Ros, R. Mathieu, N. Lugan, B. Donnadieu, *J. Organomet. Chem.* **2003**, 667, 126.
- [17] a) J. Garcia-Anton, J. Pons, X. Solans, M. Font-Bardia, J. Ros, *Eur. J. Inorg. Chem.* **2003**, 3952; b) J. Garcia-Anton, J. Pons, X. Solans, M. Font-Bardia, J. Ros, *Eur. J. Inorg. Chem.* **2003**, 2992; c) J. Garcia-Anton, J. Pons, X. Solans, M. Font-Bardia, J. Ros, *Eur. J. Inorg. Chem.* **2002**, 3319; d) J. Garcia-Anton, J. Pons, X. Solans, M. Font-Bardia, J. Ros, *Inorg. Chim. Acta* **2003**, 355, 87; e) J. Garcia-Anton, J. Pons, X. Solans, M. Font-Bardia, J. Ros, *Inorg. Chim. Acta* **2004**, 357, 571.
- [18] J. W. Steed, J. L. Atwood, in: *Supramolecular Chemistry*, Wiley & Sons Ltd., UK, **2000**.
- [19] D. C. Smith, C. H. Lake, G. M. Gray, *Chem. Commun.* **1998**, 27771.
- [20] A. Goshe, I. M. Steele, B. Bosnich, *Inorg. Chim. Acta* **2004**, 357, 4544.
- [21] The N–Pd–N–S dihedral angles decrease from 13° to 1° as we go from hexane- to nonane-chain ligands.
- [22] a) R. F. Bader, in *Atoms in Molecules. A Quantum Theory*, University Oxford Press, Oxford, **1990**; b) R. F. Bader, *Chem. Rev.* **1991**, 91, 893.
- [23] a) A. D. Becke, *J. Chem. Phys.* **1993**, 98, 5648; b) C. Lee, W. Yang, R. G. Parr, *Phys. Rev. B* **1998**, 37, 785.
- [24] M. J. Frisch, G. W. Trucks, H. B. Schlegel, G. E. Scuseria, M. A. Robb, J. R. Cheeseman, V. G. Zakrzewski, J. A. Montgomery, R. E. Stratmann, J. C. Burant, S. Dapprich, J. M. Millam, A. D. Daniels, K. N. Kudin, M. C. Strain, O. Farkas, J. Tomasi, V. Barone, M. Cossi, R. Cammi, B. Mennucci, C. Pomelli, C. Adamo, S. Clifford, J. Ochterski, G. A. Petersson, P. Y. Ayala, Q. Cui, K. Morokuma, D. K. Malick, A. D. Rabuck, K. Raghavachari, J. B. Foresman, J. Cioslowski, J. V. Ortiz, B. B. Stefanov, G. Liu, A. Liashenko, P. Piskorz, I. Komaromi, R. Gomperts, R. L. Martin, D. J. Fox, T. Keith, M. A. Al-Laham, C. Y. Peng, A. Nanayakkara, C. Gonzalez, M. Challacombe, P. M. W. Gill, B. G. Johnson, W. Chen, M. W. Wong, J. L. Andres, M. Head-Gordon, E. S. Replogle, J. A. Pople, *Gaussian 98*, Revision A.9 i A.11, Gaussian, Inc., Pittsburgh, PA, **1998**.
- [25] P. J. Hay, W. R. Wadt, *J. Chem. Phys.* **1985**, 82, 299.
- [26] a) M. J. Frisch, J. A. Pople, J. S. Binkley, *J. Chem. Phys.* **1984**, 80, 3265; b) T. Clark, J. Chandrasekhar, G. W. Spitznagel, P. v. R. Schleyer, *J. Comput. Chem.* **1983**, 4, 294.
- [27] W. J. Hehre, R. Ditchfield, J. A. Pople, *J. Chem. Phys.* **1972**, 56, 2257.
- [28] A. W. Ehlers, M. Böhme, S. Dapprich, A. Gobbi, A. Höllwarth, V. Jonas, K. F. Köhler, R. Stegmann, A. Veldkamp, G. Frenking, *Chem. Phys. Lett.* **1993**, 208, 111.
- [29] D. McQuarrie, in: *Statistical Mechanics*, Harper and Row, New York, **1986**.
- [30] A. Klamt, G. Shürmann, *J. Chem. Soc., Perkin Trans. 2* **1993**, 799.
- [31] F. Weinhold, J. E. Carpenter, in: *The Structure of Small Molecules and Ions*, Plenum, New York, **1988**.
- [32] Xaim was developed by J. C. Ortiz and C. Bo, University of Rovira i Virgili, Tarragona, Spain. Xaim is available free from <http://www.quimica.urv.es/XAIM>

Received: September 8, 2005

Published Online: November 21, 2005